Check for updates

Received: 22 October 2024 | Accepted: 9 December 2024

DOI: 10.1111/eos.13033

European Journal of Oral Sciences | NOF Scandinavian Division IADR | WILEY

ORIGINAL ARTICLE

Effect of changing the internal structure on the mechanical properties of three-dimensional-printed custom tray material: An in vitro study

Cafer Anıl Erdem | **Selin Çelik Öge** | **Orhun Ekren**

Faculty of Dentistry, Department of Prosthodontics, Çukurova University, Adana, Turkey

Correspondence
Selin Çelik Öge, Çukurova University, Faculty of Dentistry, Department of Prosthodontics, Adana, Turkey.
Email: selincelik@cu.edu.tr

Funding information
Cukurova University Scientific Research Project Coordination Unit, Grant/Award Number: TDH-2022-15048

Abstract

The main challenges to the widespread clinical application of three-dimensional (3D)-printed customized trays include cost and time limitations. This study examined how changing the internal structure of 3D-printed materials used for customized trays affects flexural strength (FS), flexural modulus (FM), manufacturing time, and material weight. Specimens (64 × 10 × 3.3 mm) were printed using a light-sensitive liquid resin. The internal structures of control specimens were completely filled, whereas the internal structures of test groups comprised vertical bars spaced 1 mm (Test 1) or 2 mm (Test 2) apart. Specimens were weighed and then subjected to a three-point bending test to evaluate their FS and FM. Data were analyzed using one-way ANOVA and Tukey's test, with Weibull analysis applied to FS values. Control specimens had the highest FS (106 ± 4 MPa), while Test 2 specimens demonstrated the highest FM (6101 ± 1407 MPa). No significant differences were found between Test 1 and Test 2 specimens in FS or FM. Test 2 specimens had the lowest mean weight (1440 ± 42 mg). Manufacturing times were 80 min for control and Test 1 specimens and 60 min for Test 2 specimens. Including spaces in the internal structure of 3D-printed custom tray material saves material and manufacturing time while maintaining mechanical properties.

KEYWORDS
dental impression technique, flexural modulus, flexural strength, three-dimensional printing

INTRODUCTION

Conventionally, dental laboratory technicians manufacture customized trays using diagnostic molds. This method is time-consuming and requires a substantial amount of laboratory work. Obtaining a diagnostic impression generally demands an additional visit, which delays the prosthetic procedure [1]. In recent years, digital technology, such as additive manufacturing, which is usually referred to as three-dimensional (3D) printing in dentistry, has offered new possibilities for producing patient-specific individual impression trays [2–4].

The utilization of a 3D-printed custom tray is an effective alternative to the traditional custom tray and should be considered for dental procedures [5]. Custom trays produced using a 3D printer have demonstrated superior performance in terms of texture matching, accuracy, and personalization compared with conventionally made trays [1, 6]. Impressions

© 2025 Scandinavian Division of the International Association for Dental Research. Published by John Wiley & Sons Ltd.

can be taken with greater precision when the space provided to the impression material is more homogenous, as this reduces deviations [1]. Although customized trays manufactured using 3D printers offer many advantages, their major drawbacks include lengthy production times and high costs, and these may prevent their widespread use.

Previous studies in several fields have reported on how changing the internal structure of different materials might decrease manufacturing times and save costs. Ekren et al. [7] performed a study to establish the internal structure of laser-sintered cobalt-chromium (Co-Cr) tensile test specimens. The specimens included cavities that suggested a structure mimicking a cage. Thus, they achieved both their objectives of saving material and achieving minimal mechanical requirements. Kocak et al. [8], on the other hand, included similar cavities within the framework of metal–ceramic restorations and determined that modifying the internal structure of such metal frameworks not only reduces their weight but also has no effect on the flexural strength (FS) and the flexural modulus (FM) of the specimens. Chen et al. [9] investigated the impact of using hollow designs on the accuracy and precision of models manufactured by 3D printers. Their findings indicated no decrease in the accuracy or the precision of a model with a hollow interior structure. Similarly, Mohammed et al. [10] demonstrated that including custom-designed void structures inside the internal architecture of 3D printed Co–Cr materials enhances its FS while simultaneously reducing its weight. The challenges to the widespread clinical use of 3D-printed customized trays are mostly time and cost constraints. Considering these findings, we speculate that integrating hollow structures into these trays may improve their utilization in clinics by decreasing production time and costs. However, there is a lack of studies on this particular topic in the current literature.

The aim of this study was, therefore, to evaluate how changing the internal structure of specimens prepared using custom tray resin for a 3D printer affects the FS, FM, weight, and production time of these specimens. The null hypothesis of the study was that changing the internal structure of the custom tray specimen has no effect on FS, FM, weight, and production time.

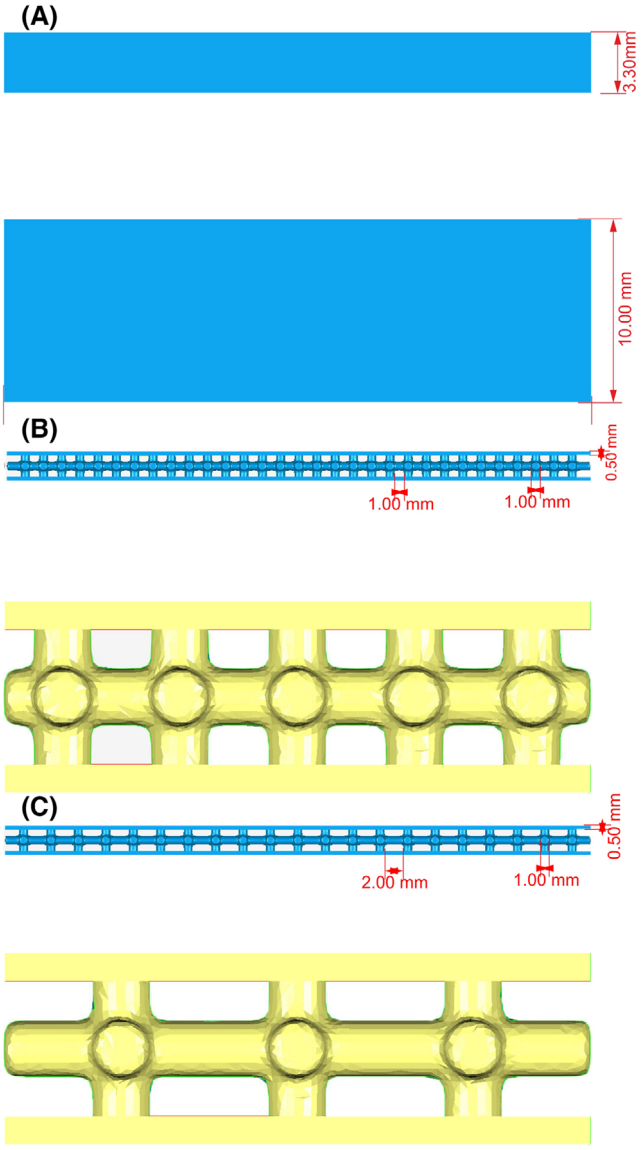


FIGURE 1 (A) Dimensions of completely full control group specimens. (B) Illustration of the cross-sectional areas of specimens from the Test 1 group, including 1-mm spaces between the vertical bars in the interior architecture. (C) Illustration of the cross-sectional areas of specimens from the Test 2 group, including 2-mm spaces between the vertical bars in the interior architecture.

MATERIAL AND METHODS

The present study was designed to conform with the Checklist for Reporting In-vitro Studies (CRIS) guidelines [11]. First, a power analysis was conducted to determine the sample size required for an experiment comprising three groups, the results of which were to be analyzed using a three-group one-way ANOVA (G*POWER V.3.1, *F*-test, fixed effect, omnibus, one-way) assuming an effect size (Cohen's *f*) of 0.5, $\alpha = 0.05$, and power = 0.80. This calculation resulted in a minimum total sample size of 42 specimens, that is, 14 per group.

In accordance with ISO 20795-1:2013 specifications, all specimens were created using a computer aided design (CAD) software application (AutoCAD, Autodesk) to have the dimensions of 64 × 10 × 3.3 mm. Control specimens were designed as compact specimens (Figure 1A); the first group of specimens (Test 1) consisted of vertical bars spaced 1-mm apart and linked by horizontal bars within the sample (Figure 1B); and in the second group of specimens (Test 2), the spacing between the vertical bars was increased to 2 mm,

16000722, 0, Downloaded from https://onlinelibrary.wiley.com/doi/10.1111/eos.13033 by Cukurova University, Wiley Online Library on [08/01/2025]. See the Terms and Conditions (https://onlinelibrary.wiley.com/terms-and-conditions) on Wiley Online Library for rules of use; OA articles are governed by the applicable Creative Commons License

and, as for Test 1 specimens, the vertical bars were linked together by horizontal bars (Figure 1C). In both test groups, the diameter of the vertical bars was 1 mm and their height was 2.3 mm. The data were saved in STL format and sent to a stereolithography (SLA) 3D printer (Form 3B, Formlabs) for printig using light-sensitive liquid resin (Custom Tray Resin, Formlabs). A total of 15 specimens from each group were printed. The light source used had a wavelength of 405 nm and 250 mW laser with an 85 μm spot size. The specimens were positioned on the build platform of the 3D printer at a 45° angle to minimize residual resin accumulation between layers and to avoid the supports intersecting with the vertical bars, and were produced with a layer thickness of 200 μm. During the manufacturing process of the specimens, each group was positioned on the 3D printer's building platform in a single session, with all specimens of each group being manufactured simultaneously.

Following printing, the specimens were cleaned using washing equipment (Form Wash, Formlabs) with 99% isopropanol. Subsequently, the specimens were polymerized using a UV curing unit (Form Cure, Formlabs) at a temperature of 60°C for 30 min.

The 3D printer provides documented manufacturing timings during the production process. The accuracy of these times was further validated using an electronic stopwatch. Following preparation of the specimens, an online randomization program (www.randomizer.org) was employed to randomize the mechanical testing order. Before the three-point bending test, the weight of each specimen was measured using an electronic balance (AX120, Shimadzu).

The specimens were tested using a universal test device (AT-M500 25 kN; Testometric) with a load cell of 250-kg force (DBBMTCL-250 kg, Ser no 27,281, Testometric) for the three-point bending test. The central location of the specimens was measured using a digital caliper (Vernier Caliper, Mitutoyo) and marked. Force was applied a speed of 5 ± 1 mm/min at the central location of the specimens until the force/deflection curve reached at peak and began to decline. No fracture was observed for any of the specimens. The force at peak values was recorded. The cross-sectional area of the specimens with a changed internal structure was calculated using 3D software (CAD SOLIDWORKS PREMIUM, Dassault Systèmes Solidworks). The calculation involved subtracting the cross-sectional areas of the hollow spaces from the total area for the Test 1 and Test 2 group specimens. Based on these adjustments, the 3D software determined the w (width) and h (height) values to be used in the FS and FM formulas for these groups. The 3D software calculated the dimensions as $w = 8.93$ mm and $h = 2.94$ mm for specimens in the Test 1 group and $w = 8.4$ mm and $h = 2.8$ mm for specimens in the Test 2 group. The FS and the FM were calculated using the following formulas:

$$\mathrm{FS} = 3PL/2wh^2$$

and

$$\mathrm{FM} = L^3P/4wh^3d,$$

where L represents the space between the two supports (in millimeters), w indicates the width; h represents the height of the specimen (in millimeters), d represents the deflection (in milimeters) induced by the force applied at the center of the structure, and P represents the force at peak value (N).

The test specimens for each group were created in a single session, so it was not feasible to conduct a statistical comparison of the manufacturing times. The FS, FM, and weight data of the specimens were analyzed using one-way ANOVA, followed by Tukey's test ($\alpha = 0.05$, IBM SPSS STATISTICS V21.0). A supplementary Weibull analysis was performed to validate the findings of the FS test, and the Weibull moduli were calculated.

RESULTS

The mean and SD values of FS, FM, and weight of the specimens are presented in Table 1. The mean FS was statistically significantly lower in Test 1 specimens than in control specimens (mean difference, Test 1 − Control = −24 MPa, 95% CI: −30 to −18) and in Test 2 specimens than in control specimens (mean difference, Test 2 − Control = −20 MPa, 95% CI: −25 to −15). No statistically significant differences in FS were observed between Test 1 and Test 2 specimens (mean difference, Test 2 – Test 1 = 4 MPa, 95% CI: −3 to 11).

The FM values were highest among Test 2 specimens (mean = 6101 MPa) and lowest among Test 1 specimens (mean = 5372 MPa) but did not differ statistically significantly between the three groups (Table 1).

The mean weight of specimens was highest in the control group (mean = 2618 mg) and lowest in the Test 2 group (mean = 1440 mg). The design of Test 1 specimens resulted in a weight that was 783 mg (95% CI: −823 to −742) lower than the weight of control specimens, while the design of Test 2 specimens resulted in a weight that was 1178 mg (95% CI: −1201 to −1155) lower than that of control specimens.

The Weibull graph for test specimens is presented in Figure 2. According to Weibull data, the control group exhibited the highest Weibull modulus ($m = 30.9$). Specimens of the Test 2 design exhibited a Weibull modulus that was lower than that of the control group ($m = 12.1$), while specimens of the Test 1 design exhibited a Weibull modulus that was lower than specimens of the Test 2 design ($m = 8.8$).

The fabrication time needed according to specimen design was 80 min for control specimens and specimens of the Test 1 design, but 60 min for specimens of the Test 2 design.

16000722, 0, Downloaded from https://onlinelibrary.wiley.com/doi/10.1111/eos.13033 by Cukurova University, Wiley Online Library on [08/01/2025]. See the Terms and Conditions (https://onlinelibrary.wiley.com/terms-and-conditions) on Wiley Online Library for rules of use; OA articles are governed by the applicable Creative Commons License

TABLE 1 Flexural strength (FS), flexural modulus (FM), and weight of the three specimen configurations.

	Specimens			Specimen comparisons		
Variable	**Control**	**Test 1**	**Test 2**	**Test 1 − Control**	**Test 2 − Control**	**Test 2 − Test 1**
FS (MPa)	106 (4)[a]	82 (11)[b]	86 (8)[b]	−24 (−30 to −18)	−20 (−25 to −15)	4 (−3 to 11)
FM (MPa)	5860 (1078)[a]	5372 (1062)[a]	6101 (1407)[a]	−488 (−1288 to 312)	241 (−696 to 1178)	729 (−203 to 1661)
Weight (mg)	2618 (14)[a]	1835 (76)[b]	1440 (42)[c]	−783 (−823 to −742)	−1178 (−1201 to −1155)	−395 (−441 to −349)
Manufacturing time (min)	80	80	60	–	–	–

Note: Different letters in the same row of rows 1–3 indicate a statistically significant difference between groups ($p \leq 0.05$).
Values are given as mean (SD) (columns 2–4, rows 1–3), mean (95% CI) (columns 5–7, rows 1–3), or min (row 4).

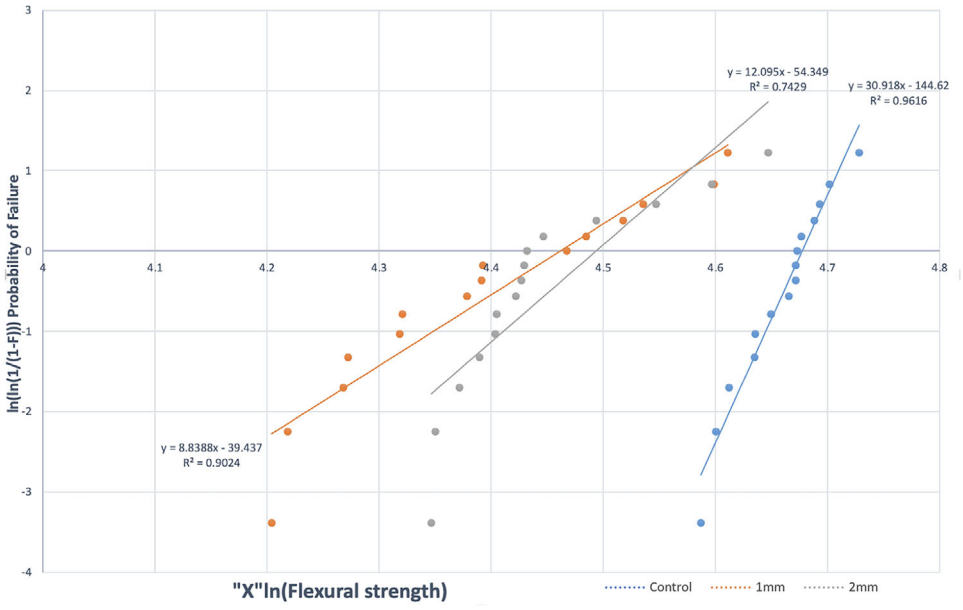


FIGURE 2 Weibull graph. *x*-axis: ln(flexural strength), *y*-axis: probability of failure, $\ln(\ln(1/(1-F)))$.

DISCUSSION

The aim of this in vitro study was to evaluate the effect of changing the internal structure of 3D-printed specimens used in manufacturing customized trays on the FS, FM, manufacturing time, and weight of the material. The study results indicated that the FS and the weight were lower for the two test designs (and more so for Test 2) than for the controls, whereas no effect of design was observed on the FM. The manufacturing time was shorter for Test 2 specimens than for Test 1 and control specimens.

There is an absence of research in the literature regarding changes in the internal structure of customized trays fabricated using 3D printers. Consequently, the FS and FM data could not be compared with results from prior research. However, according to ISO 20795-1:2013 standards, the FS for polymer-based materials should be at least 65 MPa and the FM should be at least 2000 MPa. As expected, in the present study a lower mean FS was found in Test 1 and Test 2 specimens than in control specimens, attributable to the removal of material for creating the internal lattice designs. Nevertheless, the FM remained unaffected by the changes in the internal structure. The design of the cages, created from hollowed-out specimens, affects the distribution of incoming forces within the material and impacts its mechanical strength. Still, in the present study, specimens of both test designs (Test 1 specimens: FS = 82 ± 11 MPa, FM = 5372 ± 1062 MPa; Test 2 specimens: FS = 86 ± 8 MPa, FM = 6101 ± 1407 MPa) met the minimum values required according to ISO 20795-1:2013 standards.

Liu et al. [1] performed a comparison between the FS of customized trays made using a 3D printer and those

16000722, 0, Downloaded from https://onlinelibrary.wiley.com/doi/10.1111/eos.13033 by Cukurova University, Wiley Online Library on [08/01/2025]. See the Terms and Conditions (https://onlinelibrary.wiley.com/terms-and-conditions) on Wiley Online Library for rules of use; OA articles are governed by the applicable Creative Commons License

made using conventional methods. They reported that the FS of customized trays produced using a 3D printer was 112.7 ± 1.62 MPa, whereas conventionally manufactured trays had a FS of 104 ± 2.17 MPa. In the present study, the FS values of the control group samples with solid specimens were 106 ± 4 MPa. While these values may be regarded as comparable, the discrepancy may arise from the utilization in the study by Liu et al. [1] of a 3D printer employing a different technology (fused deposition modeling) and a layer thickness of 400 μm during manufacturing.

Liu et al. [12] conducted a study to evaluate how the thickness of the layers affects the mechanical properties of 3D-printed customized trays. They found that the FS of the specimens created with a layer thickness of 200 μm, which is the same as that used in the present study, was approximately 125 MPa. The specimen dimensions and test procedure were the same in both investigations. However, Liu et al. [12] used a 3D printer with fused deposition modeling technology and a resin with different chemical compositions for manufacturing their specimens, whereas, in the present study, a 3D printer with SLA technology was used. In addition, Liu et al. [12] selected 0° as the build angle, which also contrasts with the build angle of 45° used in the present study. These may be potential explanations for the different outcomes.

Weibull analysis is a statistical method commonly employed in different fields, such as engineering, materials science, health, and economics. The objective of Weibull analysis is to create a model that can predict the time frame of an event. A low Weibull modulus indicates a wide distribution of values and high variability in measurements, whereas a high Weibull modulus indicates a narrow distribution of values and low variability. In the present study, the *x*-axis of the Weibull graph denotes ln(flexural strength), whereas the *y*-axis indicates the probability of failure, represented as $\ln(\ln(1/(1-F)))$ (Figure 2). This graph illustrates the distribution of FS values and the material's reliability, offering insights into its mechanical performance and consistency. The control group exhibited the highest Weibull modulus ($m = 30.9$), whereas Test 1 specimens exhibited the lowest Weibull modulus ($m = 8.8$). Given these conditions, it might be preferable to choose tray production with a 2-mm spacing (i.e., the Test 2 design). Therefore, it is possible to create impression trays that are both clinically acceptable and predictable, possessing adequate mechanical strength for use in clinical settings, while also saving on material and time.

When analyzing the FS values of the test groups in the study, it was noted that there was no significant difference between the test groups. Furthermore, while considering the ecological perspective, the Test 2 design used less material than the Test 1 design. Simultaneously, the manufacture of Test 2 specimens required 25% less time than the manufacture of Test 1 specimens. This led the authors to speculate that utilizing a customized tray material with 2-mm spaces between the vertical bars in the architecture, the mechanical properties of which are also consistent with the standards, is a feasible option in terms of time and cost savings. The higher the FM, the higher the resistance of the material to bending (high rigidity). This property is very important, especially if multiple implant impressions are to be taken with silicone elastomers. The rigidity of the tray prevents the impression material from deforming excessively during removal from the mouth and thereby ensures passive fit of the restoration. Although no statistically significant difference was found in terms of the FM among groups, slightly higher values among Test 2 specimens further encourage the authors to recommend the Test 2 design for clinical practice.

As presented in the Material and Methods section, the values of FS and FM of the test specimens were calculated by formulas utilizing a peak force provided by the testing equipment. The width and height of all test specimens may not be the same because of voids in the cross-sections of Test 1 and Test 2 designs. We therefore decided to measure the precise width and height measurements of the specimens from Test 1 and Test 2 groups that were different from those of the control group, in order to calculate FS and FM through the use of a dedicated software program as recommended by Kocak et al. [8] specifically for laser-sintered Co–Cr metal frameworks with a modified internal structure. Furthermore, Ekren et al. [7] demonstrated that calculating the correct cross-sectional area leads to more accurate outcomes when evaluating mechanical properties.

In conclusion, the findings of the present study indicate that the Test 2 design described here is the most optimal design regarding price/performance as it minimizes production time and costs while maintaining mechanical strength. Additionally, utilizing this design enables the preparation of trays with essential properties for precise impressions, yielding benefits in both cost and time. The dimensional stability, precision, and bonding of the impression material to the tray are also crucial to the mechanical strength of the tray material [12–14]. The implementation of this manufacturing technique is mechanically feasible, but further studies are required to investigate the bonding of 3D-printed customized trays with a changed internal structure to the impression material, as well as to evaluate accuracy and dimensional stability. Also, it should be noted that the study has limitations in terms of statistical comparison of manufacturing periods due to the fact that the test specimens for each group were produced in a single session.

AUTHOR CONTRIBUTIONS

Conceptualization: Orhun Ekren. **Formal analysis:** Orhun Ekren. **Investigation:** Cafer A. Erdem. **Methodology**: Orhun Ekren and Cafer A. Erdem. **Project administration**: Orhun Ekren. **Resources:** Selin Ç. Öge. **Writing—original draft:** Selin Ç. Öge. **Writing—review and editing:** Orhun Ekren.

16000722, 0, Downloaded from https://onlinelibrary.wiley.com/doi/10.1111/eos.13033 by Cukurova University, Wiley Online Library on [08/01/2025]. See the Terms and Conditions (https://onlinelibrary.wiley.com/terms-and-conditions) on Wiley Online Library for rules of use; OA articles are governed by the applicable Creative Commons License

ACKNOWLEDGMENTS

This study was presented as an oral presentation at the Cukurova University, Faculty of Dentistry International Dental Congress on Additive Manufacturing (IDCAM 2024), which was held from May 30 to June 1, 2024, in Adana, Turkey. This study was supported by the Cukurova University Scientific Research Project Coordination Unit (Project ID: TDH-2022-15048).

CONFLICT OF INTEREST STATEMENT

The authors declare no conflicts of interest.

ORCID

Cafer Anıl Erdem https://orcid.org/0000-0002-0530-325X
Selin Çelik Öge https://orcid.org/0000-0003-1403-6832
Orhun Ekren https://orcid.org/0000-0002-3237-8003

REFERENCES

1. Liu Y, Di P, Zhao Y, Hao Q, Tian J, Cui H. Accuracy of multi-implant impressions using 3D-printing custom trays and splinting versus conventional techniques for complete arches. Int J Oral Maxillofac Implants. 2019;34:1007–14.
2. Tian Y, Chen CX, Xu X, Wang J, Hou X, Li K, et al. A review of 3D printing in dentistry: technologies, affecting factors, and applications. Scanning. 2021;2021: 9950131. https://doi.org/10.1155/2021/9950131
3. Jockusch J, Özcan M. Additive manufacturing of dental polymers: an overview on processes, materials applications. Dent Mater J. 2020;39:345–54.
4. Balhaddad AA, Garcia IM, Mokeem L, Alsahafi R, Majeed-Saidan A, Albagami HH, et al. Three-dimensional (3D) printing in dental practice: applications, areas of interest, and level of evidence. Clin Oral Investig. 2023;27:2465–81.
5. Yang X, Liu Y, Li Y, Zhao Y, Di P. Accuracy and feasibility of 3D-printed custom open trays for impressions of multiple implants: a self-controlled clinical trial. J Prosthet Dent. 2022;128:396–403.
6. Kim JE, Park JH, Kim JH, Shim JS. Computer-based implant planning involving a prefabricated custom tray with alumina landmark structures. J Prosthet Dent. 2019;121:373–7.
7. Ekren O, Kocak EF, Ucar Y. Effect of internal design changes on the mechanical properties of laser-sintered cobalt-chromium specimens. J Prosthet Dent. 2023;129:508–12.
8. Kocak EF, Ekren O, Ucar Y. Effect of internal design modification on the mechanical properties of laser sintered cobalt-chromium multi-unit metal-ceramic frameworks. J Prosthodont. 2022;31:766–70.
9. Chen Y, Li H, Zhai Z, Nakano T, Ishigaki S. Impact of internal design on the accuracy of 3-dimensionally printed casts fabricated by stereolithography and digital light processing technology. J Prosthet Dent. 2023;130:381.e1–7. https://doi.org/10.1016/j.prosdent.2023.06.029
10. Mohammed AJ, Al-Ali AA. The influence of internally architected voids in the creation of high-strength, low-weight 3D-printed cobalt-chromium prototypes. Dent Res J. 2024;21:21. https://doi.org/10.4103/drj.drj_627_23
11. Krithikadatta J, Gopikrishna V, Datta M. CRIS guidelines (checklist for reporting in-vitro studies): a concept note on the need for standardized guidelines for improving quality and transparency in reporting in-vitro studies in experimental dental research. J Conserv Dent. 2014;17:301–4. https://doi.org/10.4103/0972-0707.136338
12. Liu Y, Bai W, Cheng X, Tian J, Wei D, Sun Y, et al. Effects of printing layer thickness on mechanical properties of 3D-printed custom trays. J Prosthet Dent. 2021;126:671.e1–7. https://doi.org/10.1016/j.prosdent.2020.08.025
13. Burns J, Palmer R, Howe L, Wilson R. Accuracy of open tray implant impressions: an in vitro comparison of stock versus custom trays. J Prosthet Dent. 2003;89:250–5.
14. De Avila ED, Castanharo SM, Casalle N, Vasconcelos JA, Mollo FDA. Effect of the association between the tray and impression techniques on angulated implants using the all-on-four system. J Oral Implantol. 2015;41:382–5.

How to cite this article: Erdem CA, Çelik Öge S, Ekren O. Effect of changing the internal structure on the mechanical properties of three-dimensional-printed custom tray material: An in vitro study. Eur J Oral Sci. 2025;e13033. https://doi.org/10.1111/eos.13033

16000722, 0, Downloaded from https://onlinelibrary.wiley.com/doi/10.1111/eos.13033 by Cukurova University, Wiley Online Library on [08/01/2025]. See the Terms and Conditions (https://onlinelibrary.wiley.com/terms-and-conditions) on Wiley Online Library for rules of use; OA articles are governed by the applicable Creative Commons License